Appl. Phys. B 46, 347–355 (1988)

Applied Physics B Photophysics and Laser Chemistry

Frequency and Time Resolved Luminescence of Intermediate Reaction Products in ir Laser Decomposition of Silane

E. Borsella and L. Caneve*

ENEA, Dip. TIB, U.S. Fisica Applicata, CRE Frascati, C.P. 65, I-00044 Frascati, Rome, Italy

Received 2 July 1987/Accepted 3 November 1987

Abstract. A systematic study of spectral and time dependence of the luminescence emitted by fragments after ir multiple-photon decomposition of silane is presented. Data obtained at various silane pressures (1–35 Torr) and pulsed CO_2 laser fluences are discussed and compared with previous results and interpretations.

PACS: 82.50Et, 33.80Wz

The monosilane decomposition process has received much attention and growing interest in the last few years due to the possibility of polycrystalline, amorphous and amorphous-hydrogenated silicon (α-Si:H) deposition.

In spite of several successful applications [1–3] the silane decomposition mechanism is not yet clear.

A long debate started in 1966 [4] on the primary dissociation step. Initiation of silane pyrolysis was attributed to the homogeneous reaction:

$$SiH_4 \rightarrow SiH_2 + H_2 \quad (1)$$

while a gas phase reaction leading to $SiH_3 + H$ was discarded on the basis of thermochemistry [4]. However, in a recent paper [5], Robertson et al. claimed that silane decomposition is a heterogeneous process initiated by wall reactions involving deposits of α-Si.

Several papers have been written in the last years [6–9] which discuss the reaction dynamics of gas phase silane decomposition. Many of the proposed models are based on final product analysis, thus overriding the chemical reactions which occur during the initial stages of the process.

In our opinion, a conclusive reaction mechanism has not yet been elucidated and spectroscopic detection of early reaction products can help in shedding light on this subject. To this end, we performed a detailed study of the spectral and temporal dependence of fragment luminescence after ir multiple-photon dissociation of SiH_4 excited by pulsed CO_2 laser radiation.

As pointed out by [10], distinct emissions are detected when SiH_4 is irradiated with the 10 P(20) (944 cm^{-1}) line of an unfocussed or focussed CO_2 laser. A faint emission around the laser beam path is observed visually in the first case, while a bright pink emission illuminating the whole cell is seen in the latter case [11].

However, to our knowledge, there is no systematic investigation in the literature of the spectral and temporal dependence of this luminescence.

In the following, data obtained at various silane pressures (1–35 Torr) and CO_2 laser fluences will be presented. Our results will be discussed and compared with findings reported by other investigators in this field.

1. Experimental

A scheme of the experimental set-up is shown in Fig. 1.

Silane excitation was carried out using a pulsed, multimode, line-tunable TEA CO_2 laser (Lumonics Mod. 102). The typical pulse shape consisted of a 100 ns (FWHM) peak followed by a tail of about 1.5 μs when the laser was operated with a 65:30:11

* ENEA Guest

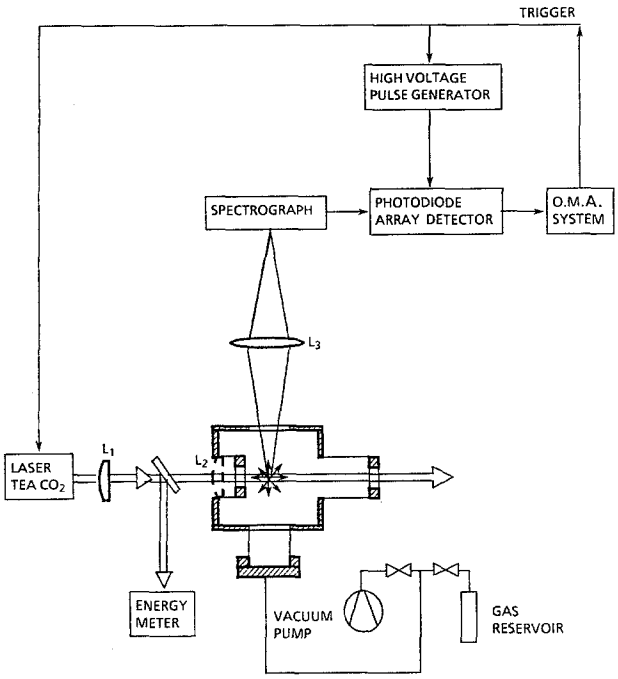

Fig. 1. Schematic of the experimental set-up

$He:CO_2:N_2$ atmospheric gas mixture. Laser energy was monitored throughout the course of the experiment by collecting on the surface of a Gen-Tec pyroelectric detector (Mod. PRJ-D) a fraction of the laser beam which was deflected by a 10% reflectivity ZnSe beamsplitter. Whenever necessary, the pyroelectric detector was replaced by a fast detector (Molectron Mod. P3) in order to acquire the laser pulse time profile. Two different optical configurations were used to focus the laser radiation into the 15 cm long cubic stainless steel reaction cell. In the *parallel* optics, the laser beam was mildly focussed in the centre of the cell by a 2 m focal length NaCl lens (L_1) which produced a collimated region of radiation along the cell axis. In this configuration, the optical entrance ZnSe window was mounted at 1 cm from the centre of the cell. The beam cross section, as measured by burnt patterns on thermosensitive paper, was equal to 0.28 cm^2 in the centre of the empty cell. Typical laser fluences were in the range 1–3 J/cm^2.

In the *focussing* optics, the entrance ZnSe cell window was replaced by an AR coated 2.5″ focal length ZnSe lens (L_2) mounted at a distance equal to the focal length from the centre of the cell. In this configuration, the laser fluence in the centre of the empty cell was about 30 J/cm^2.

High purity silane gas was supplied by *L'Air Liquid* with a stated purity of 99.999% and was used without further purification. The vacuum chamber was pumped by a 450 l/s Elettrorava (Mod. ETP 8/450) Turbomolecular pump and the background pressure was $\lesssim 10^{-5}$ Torr. The SiH_4 pressure in the cell was measured with a MKS Baratron capacitance manometer.

The visible luminescence was detected at right angles to the laser beam through a quartz window. A 12.5 cm focal length quartz lens ($\Phi = 5$ cm) collected a portion of the visible radiation and imaged it (with lateral magnification $M = 1$) on the entrance slit of a 0.32 m focal ISA spectrograph Mod. HR-320 ($f_N = 5$) supplied with a 150 grooves/mm grating.

A EG & G Optical Multichannel Analyzer (OMA III) was employed for simultaneous detection of the luminescence spectrum. An intensified silicon photodiode array detector (512 elements) was mounted at the exit of the spectrograph and the luminescence spectrum was acquired with a resolution of approximately 5 Å per channel. The sensitivity (photons/count) of the detector (EG & G 1420 BR-512-G) at three points across the spectral range (180–900 nm) is: 8 at 300 nm, 15 at 550 nm, and 67 at 830 nm. The detector was either operated with a fixed exposure time of 16 ms or gated by a high voltage pulse generator (EG & G Mod. 1211) with fast rise and fall times (a time resolution of better than 40 ns was achieved in this configuration).

When the luminescence signal was too weak to be detected by the OMA system, a RCA 1*P*28 photomultiplier was used as light detector. A rough spectral analysis was performed by use of filters ranging from 400 nm to 700 nm (with a bandwidth of about 50 nm). The photomultiplier output was fed to a digital oscilloscope (TEK 2430) with 40 MHz bandwidth for time analysis of weak luminescence signals.

2. Luminescence Arising from the ir Multiple Photon Dissociation of SiH_4 at Low CO_2 Laser Fluence

2.1. Results

When silane is irradiated with a parallel CO_2 laser beam tuned at 944.4 cm^{-1}, distinct regimes can be observed in the spectral and time dependence of the total emission at silane pressures ranging from 1 to 35 Torr.

At silane pressures in the range 1–12 Torr, the total luminescence consists of two different components (Fig. 2). The fast one has a lifetime of 180 ± 20 ns and is delayed of 80 ns with respect to the maximum of the laser pulse. The slow one has a lifetime of about 0.9 μs and a delay of ~400 ns. These delay times are not sensitive to changes in the laser fluence and gas pressure. The maximum intensity of both components of the total emission increases linearly vs. silane pressure, as shown in Fig. 3a. Due to the low intensity of the luminescence, in these experimental conditions

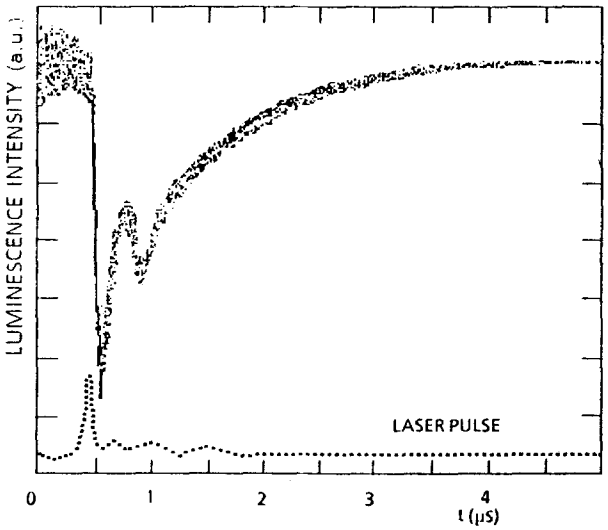

Fig. 2. Time dependence of fragment emission at $p(SiH_4)$ = 7 Torr; $\Phi \simeq 2.5$ J/cm^2

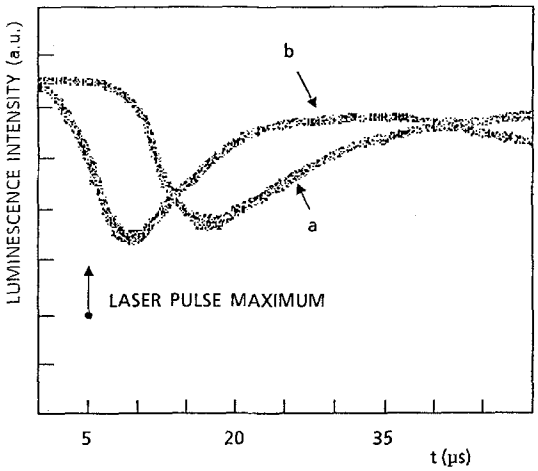

Fig. 4. Time dependence of fragment luminescence at $p(SiH_4)$ = 20 Torr: *a* $\Phi \approx 1.5$ J/cm^2, *b* $\Phi \approx 2$ J/cm^2

spectral analysis was performed with filters ranging from 400 nm to 700 nm (with a bandwidth of ~ 50 nm). The emission falls in the range 550–700 nm, being centered at about 650 nm. Both the time components are detected in the whole emission wavelength range.

As shown in Fig. 3b, the total luminescence intensity increases dramatically above 20 Torr and shows a tendency towards saturation at pressures greater than 35 Torr. The time dependence of the total chemiluminescence signal at 20 Torr is shown in Fig. 4 for two different laser fluences. Very long decay and rise times are found, which turn out to be quite sensitive to changes in laser energy. Spectral analysis of the luminescence emitted at pressures above 20 Torr was performed with the Optical Multichannel Analyzer (OMA). The emission spectrum in the pressure range 15–35 Torr consists of two broad bands peaking at 720 nm and at 820 nm, respectively. Typical spectra, which are not corrected for the detector sensitivity, are reported in Fig. 5. The sudden decrease of luminescence intensity at $\lambda \geqq 850$ nm could be due to the detector spectral response (see Sect. 1). The spectral distribution was found almost independent on laser fluence as well as on time delay between the laser pulse maximum and the start of signal acquisition. The last result was found acquiring the emission spectrum with

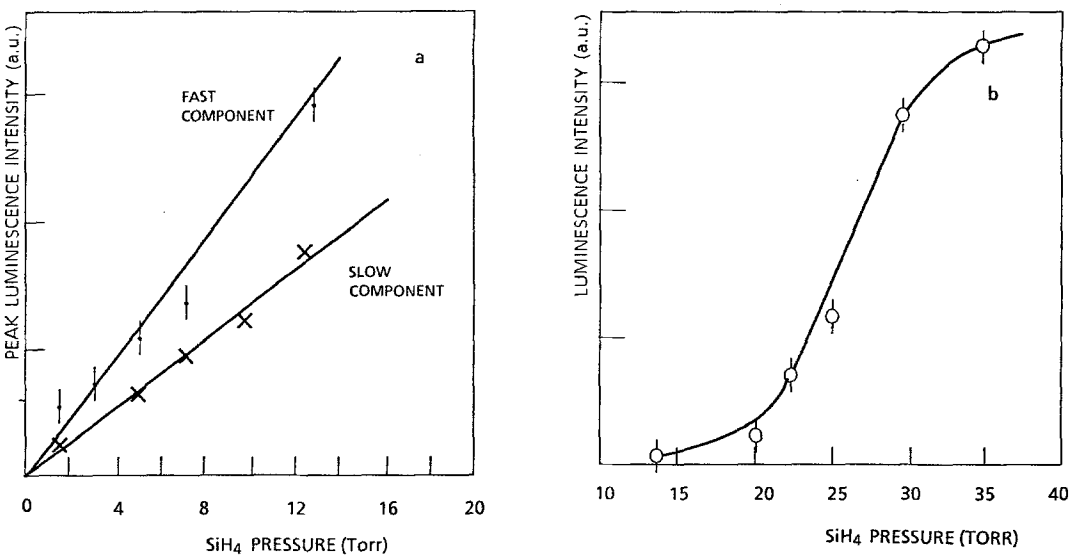

Fig. 3a, b. Luminescence intensity vs. silane pressure at $\Phi \simeq 2.5$ J/cm^2. (a) $p(SiH_4)$ in the range 1.5–12 Torr, (b) $p(SiH_4)$ in the range 14–35 Torr

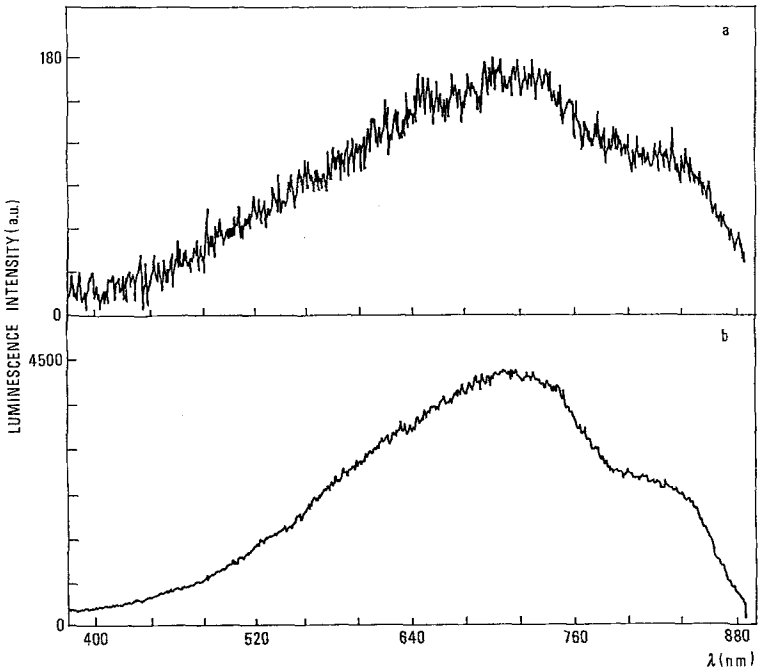

Fig. 5a, b. OMA spectrum of fragment emission after ir MPD of SiH_4 at low laser fluence $\Phi \simeq 2.5$ J/cm^2: (a) $p(SiH_4) = 20$ Torr; (b) $p(SiH_4) = 30$ Torr

a fixed exposure time of 500 ns at different delay times with respect to the laser pulse maximum.

At pressures above 15 Torr, a yellow-brown powdery deposit was observed after several laser shots on the walls and on the windows of the cell. As discussed in the following, the powdery deposit was mostly formed by silicon which does not appreciably absorb the CO_2 laser radiation (at 944 cm^{-1}). However, the whole cell was accurately cleaned before each set of measurements and the absence of deposit interference with the luminescence signals has been carefully checked throughout the course of the experiment.

2.2. *Discussion*

It is generally accepted that ir laser induced dissociation of a molecule A is given by the following mechanism [12]:

$$A \xrightarrow{n_1 h\nu} A^* \tag{2}$$

$$A^* \xrightarrow{n_2 h\nu} A^{**} \tag{3}$$

$$A^* + A^* \rightarrow A^{**} + A \tag{4}$$

$$A^* + A \rightarrow A + A \tag{5}$$

$$A^{**} + A \rightarrow A^* + A \tag{6}$$

$$A^{**} \rightarrow \text{products}. \tag{7}$$

Here A are the unexcited molecules, A* and A** are the vibrationally excited molecules below and above the dissociation limit, respectively.

In the low pressure regime, molecules can undergo decomposition only through the step (3), since no collisions can take place before dissociation, while in the high pressure regime two molecules with intermediate energy content A* collide to give a molecule A** which is excited above the dissociation threshold.

Infrared laser induced dissociation of polyatomic molecules is often accompanied by visible-uv luminescence from electronically excited fragments. In the collision-free limit, luminescence is expected to build up almost instantaneously with the laser pulse, the rise time being independent of substance pressure, while the luminescence intensity is expected to increase linearly with gas pressure.

On the other side, collisional activation (step 4) gives rise to a higher than linear dependence of the product luminescence on substance pressure and rise and decay times are expected to be pressure dependent.

At low laser fluences, broad and structureless emission spectra due to more than diatomic fragments should be observed, while at high laser fluences characteristic frequencies of diatomic and monoatomic species are expected to dominate the emission spectra.

Keeping in mind these considerations, we have interpreted data obtained at low laser fluence as follows.

The observed chemiluminescence has been tentatively assigned to emission from electronically excited states of SiH_2. At low pressures (<12 Torr), the emission detected in the range 550–700 nm could be ascribed to decay from $^1B_1$ electronic state to $^1A_1$ ground state of SiH_2 radical. This assignment is consistent with the absorption data reported in [13]

and will be further discussed in connection with the results obtained at SiH_4 pressure above 15 Torr. Moreover, the time dependence of the total emission at $p<12$ Torr can be discussed on the basis of the results reported in [14] about fluorescence lifetimes of individual rovibronic levels of $^1B_1$ state of SiH_2. A wide dispersion in the lifetimes of different rovibronic levels has been reported, ranging from ~ 10 ns to >10 μs. This behaviour has been ascribed to a strong perturbation of $^1B_1$ rovibronic states by mixing with $^1A_1$ and $^3B_1$ states. In our experiment SiH_2 can be formed in several excited states, thus the fast decay time of ≈ 180 ns could arise from a superposition of decay times from different $^1B_1$ rovibronic states. The experimental value of ~ 180 ns is also in reasonable agreement with the radiative lifetime of the $^1B_1$ electronic state ($\tau_{rad}=0.3$ μs) as estimated in [14] from absorption data. As for the slow component, it could be due to triplet emission from $^3B_1$ levels strongly coupled to $^1B_1$ levels. However, a more accurate spectral analysis of the luminescence emitted at $p<12$ Torr is necessary, in order to firmly establish the origin and the nature of the emitting fragment.

An interesting feature of the measurements in the low pressure regime is the approximately linear dependence of both time components on silane pressure (Fig. 3a). This linear dependence, as well as the independence on silane pressure of the luminescence onset, should be indicative of a true collisionless unimolecular decomposition [12]. Since polyatomic molecules are expected to undergo true collisionless multi-photon excitation at much lower pressures [12], further investigation is necessary in order to get full evidence for the occurrence of coherent multiphoton excitation of SiH_4. However, the V–V relaxation time of SiH_4 ($\simeq 5$ μs · Torr) [15] is longer than typical V–V relaxation times of other polyatomics (~ 1 μs · Torr for SF_6) [16] and collisionless conditions are achieved at least for SiH_4 pressure ~ 1 Torr (the CO_2 laser pulse duration being 1.5 μs).

At pressures above 15 Torr, the emission has been ascribed to decay from collisionally excited electronic states of SiH_2. The band peaking at 720 nm has been assigned to the $^1B_1 \rightarrow {}^1A_1$ transition. This identification is based on the following considerations. In [17] the energy separation between the lowest singlet ($^1B_1$) and the ground state ($^1A_1$) has been calculated to be 16936.5 cm^{-1}. By taking into account the bending vibrational frequency in the ground state $^1A_1$ (~ 1004 cm^{-1} [13]) and in the $^1B_1$ electronic state (~ 860 cm^{-1} [13]), we have verified that band emission due to the bending vibrational transitions $(0, v_2', 0) \rightarrow (0, v_2'', 0)$ should fall in the range 500–800 nm. It is the relevant difference in the equilibrium angle between the excited state (123° for $^1B_1$) [17] and the ground state (92° for $^1A_1$) [17] which makes the luminescence spectrum very broad.

On the other side, as far as it concerns the band centered around 840 nm, a proper spectral analysis is impossible due to the lack of spectroscopic data for the other electronic states of SiH_2. Further difficulties in interpreting data arise from the mixing of electronic states proposed in [15], which should lead to relevant perturbations in energy level positions. We believe that also the emission peaking at 840 cm^{-1} is ascribable to SiH_2 since it is closely related to the emission at shorter wavelengths. In fact, the shape of the emission spectrum does not change either when the gas pressure is varied in the range 15–35 Torr (Fig. 5) or when the luminescence is detected at different delay times with respect to the laser pulse maximum. In principle, a different behavior is expected for two distinct molecular species.

We have discarded the possibility that other radicals can be responsible for the chemiluminescence peaking at 840 nm, since SiH displays a well resolved structure in the range 405–420 nm [18], while the lowest energy transitions of SiH_3 lie in the uv [19]. We can also neglect the possibility of emission due to reaction products with residual O_2, since the lowest energy transitions of SiO [18] fall in the region 420–430 nm, while chemiluminescence from H_2SiO [20] falls in the range 470–650 nm and exhibits maximum intensity around 500 nm.

Finally, it is worth mentioning that SiH_2 has been identified as a photolysis product in the secondary ir multiple-photon dissociation of several organo-silanes [14, 21].

The attribution of the observed chemiluminescence to decay from electronically excited states of the sylilene radical confirms the occurrence of the homogeneous reaction (1).

It seems clear that at pressures above 15 Torr, collisional activation becomes the dominant process in inducing multiple-photon dissociation of silane. In fact a higher than linear dependence of the product luminescence on SiH_4 pressure is found, as shown in Fig. 3b. The trend of luminescence intensity at $p(SiH_4) \geqq 35$ Torr can be explained by the saturation of ir absorption (at 944 cm^{-1}) in pure SiH_4 as found by Pauleau et al. [22]. The influence of laser fluence on the time behavior of chemiluminescence at $p=20$ Torr is shown in Fig. 4. The very long rise and decay times are due to the collisional process of energy pooling [23] between molecules excited below the dissociation threshold (step 4), which provides a continuous source of electronically excited SiH_2 fragments until vibrational cooling is achieved by V–T transfer processes (step 5). The delay time between the laser pulse and the onset of luminescence (called the "incubation time") as

well as the rise of the luminescence signal should reflect the production of photofragments via V–V pumping of the parent molecule, while the fall should be determined by V–T relaxation processes. It is thus conceivable that the incubation and rise times decrease as the laser fluence increases (Fig. 4).

3. Luminescence Arising from the ir Laser Induced Dissociation of SiH_4 at High Laser Fluence

3.1. Results

When the laser radiation is focussed in the centre of the cell, a bright pink luminescence is emitted at SiH_4 pressures $\geqq 3$ Torr. Typical emission spectra consist of sharp peaks in the wavelength range 200–700 nm. Similar line optical spectra have been detected by Deutsch [11] in laser induced dissociation of SiH_4, by Steinwandel and Hoeschele [24] in the shock-wave induced decomposition of SiH_4 (at temperatures exceeding 3000 K) and, finally, by Kampas and Griffith [25] in silane glow discharge plasma experiments. The emitting species in all these experiments have been identified as H, H_2, SiH, and Si. The analogy between our spectra and optical emission in the silane glow discharge led us to the hypothesis that CO_2 laser induced silane breakdown takes place in the laser focal region. In order to check this idea, two parallel plates (with a separation of 2.2 cm) have been placed along the focal region of the CO_2 laser. Electronic or ionic current pulses (FWHM ≈ 1 μs), are detected when a potential difference of + or −50 V is set across the plates.

After having found evidence for the presence of electrons in the focussed CO_2 laser field, we are left with the problem of clarifying the mechanism of silane decomposition at high CO_2 laser fluence. In order to sort out the sequence of reactions taking place after laser irradiation, the entire luminescence spectrum has been detected at different delay times with respect to the CO_2 laser pulse maximum (Fig. 6). Fragment identification is reported in Table 1.

Table 1. Fragment identification from spectral lines of Fig. 6

Line	Wavelength (nm)	Fragment
1	243.9	Si [26]
2	251.9	Si [26]
3	263.1	Si [26]
4	288.1	Si [26]
5	298.7	Si [26]
6	381.6	H_2 [18]
7	386.3	SiH [18]
8	390.5	Si [18]
9	394.1	H_2 [18]
10	406.9	H_2 [18]
11	412.8	SiH [18]
12	434.0	H [26]
13	456.8	H_2 [18]
	457.2	
14	486.1	H_β [26]
15	505.5	H_2 [18]
16	527.2	H_2 [18]
17	548.1	H_2 [18]
18	576.2	Si (2nd order)
19	583.6	H_2 [18]
20	632.7	H_2 [18]
21	639.9	H_2 [18]
22	656.3	H_α [26]
23	781.0	Si (2nd order)

The time dependence of fragments emission is reported in Fig. 7 for selected lines of SiH, H_2, Si, and

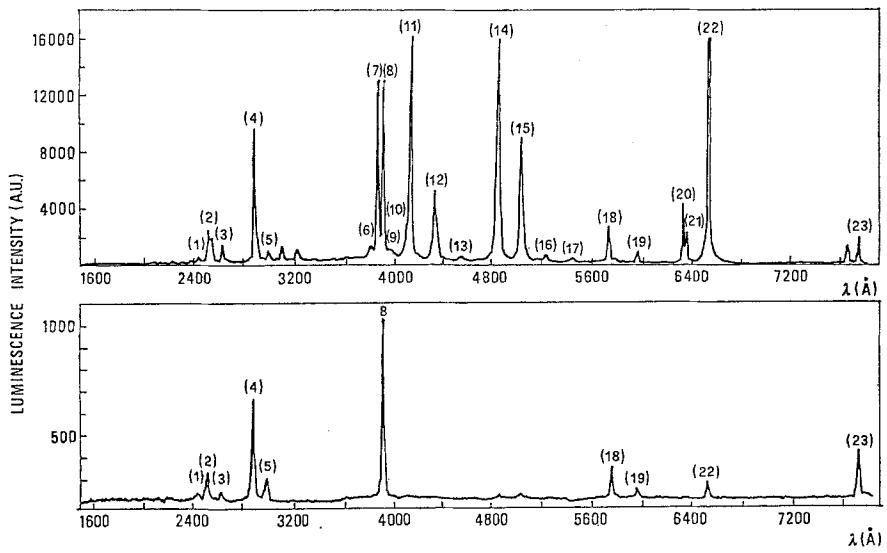

Fig. 6a, b. OMA spectra of fragment emission after ir MPD of SiH_4 ($p = 5$ Torr) with the focussed TEA CO_2 laser output: (a) delay time: 150×10^{-8} s, exposure time: 50×10^{-8} s; (b) delay time: 6×10^{-6} s, exposure time 8×10^{-6} s

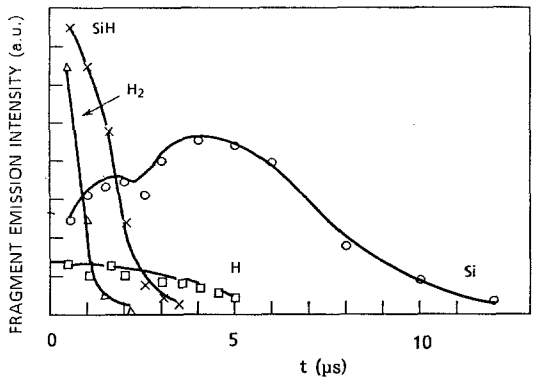

Fig. 7. Photofragment emission intensity following SiH_4 irradiation with the focussed CO_2 TEA laser output. The measurements were done at different delay times with respect to the laser pulse maximum. The exposure time was fixed at 50×10^{-8} s

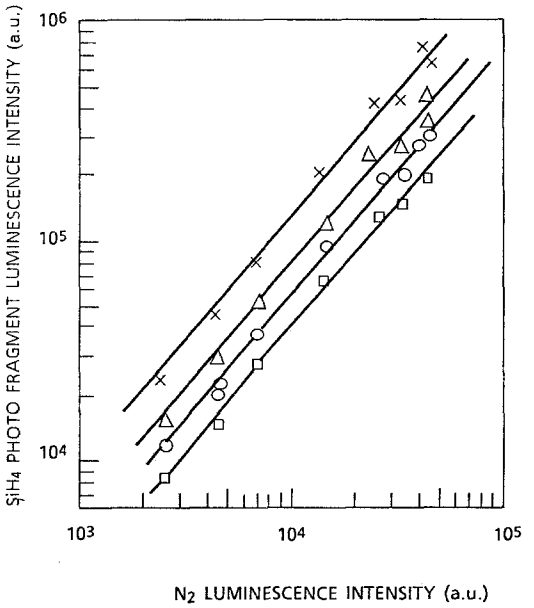

Fig. 8. Plots of the SiH_4 photofragment emission intensities vs. the emission intensity of N_2 for the same CO_2 laser power: (×)=SiH; (△)=H_2; (○)=Si; (□)=H

H. A fixed exposure time of 500 ns was used throughout this series of measurements. It comes out that emission from SiH and H_2 excited photo-fragments ends within the first few microseconds, while emission from H and Si excited states last for about 5 μs and 12 μs, respectively.

In order to identify which fragments are primary products of silane decomposition, we added a small fixed quantity of nitrogen to silane (in the ratio 1 : 5) and monitored the emission from Si, SiH, H, H_2, and N_2 as a function of CO_2 laser intensity. Formation of emitting excited states of N_2 require only one electron, therefore emission from excited primary products of silane decomposition is expected to be proportional to the emission intensity of N_2 excited fragments when the CO_2 laser field intensity is increased [25].

Experimental results reported in Fig. 8 show that the ratio between silane and N_2 fragment emission intensity is roughly independent on CO_2 laser discharge for all the excited species. All the emitting fragments should therefore be primary products of silane decomposition.

3.2. Discussion

It is clearly evident that a different decomposition mechanism is involved at very high CO_2 laser fluences. The origin of diatomic and monoatomic emitting fragments will be discussed in the following. Appearance potentials for emission from excited fragments of SiH_4 have been measured by electron impact dissociation (see [27]). The experimentally found values are 10.5 eV, 11.5 eV and 20 eV for SiH, Si, and H Balmer emission, respectively, thus electrons with energies higher than 20 eV are produced in the CO_2 laser focal region.

The energetically allowed silane dissociation pathways are reported in [28]. The appearance potentials below the 1st IP (ionization potential) of silane (12.8 eV) [29] are consistent with the following dissociation channels [28]:

$$SiH_4 + e^- \rightarrow SiH(A^2\Delta) + H_2(X^1\Sigma_g^+) + H(1^2S) \quad (8.6\text{ eV})$$

$$SiH_4 + e^- \rightarrow Si(4s\,^3P_0) + 2H_2(X^1\Sigma_g^+) \quad (9.5\text{ eV})$$

$$\rightarrow Si(4s\,^1P_0) + 2H_2(X^1\Sigma_g^+) \quad (9.6\text{ eV})$$

Emission from $SiH(A^2\Delta)$ [18], $Si(^3P_0)$ [26], and $Si(^1P_0)$ [26] excited fragments is observed in the spectra reported in Fig. 6. In the energy range above the 1st IP, superexcited states of silane can be formed, which are characterized by a Rydberg nature (see [27, 28]). In fact, when an excitation energy E greater than the 1st IP is transferred to the molecule, a ground state electron can be promoted to a level of a Rydberg series converging to a higher ionization limit. The Rydberg electron behaves as a spectator orbiting at a large distance from the nuclei, while the remainder of the molecule determines the final dissociative processes [28, 30]. When the parent molecule dissociates, the Rydberg electron can be captured by the positively charged ion entering one of its Rydberg orbitals, otherwise dissociative ionization takes place.

Autoionizing Rydberg series converging to the second ionization limit (near 18 eV) [29] of SiH_4 have been observed in threshold photoelectron spectroscopy [31] and large angle electron scattering [32] experiments. More recently autoionization structure following resonant excitation of Rydberg states con-

verging to the 2nd ionization limit of SiH_4 has been detected by Börlin et al. [33] in the photoionization cross section of all the SiH_4 ions between 15.5 eV and 18 eV.

If dissociation from superexcited states into neutral fragments takes place, emission is observed when the Rydberg electron cascades down to some lower state of the fragment. Optical emission from neutral fragments after dissociation of SiH_4 superexcited states has been observed by Perrin and Aarts [27] in e-impact experiments. The AP for H Balmer emission has been found at 19 eV and a second onset for Si ($4s\,^1P_0$) emission has been found at 20 eV. In analogy with the experiment of Perrin and Aarts, we suggest that H Balmer emission and a contribution to Si emission in the spectra reported in Fig. 6 is due to deexcitation of metastable, high-lying Rydberg states of H and Si formed after dissociation of superexcited states of silane. This hypothesis is furtherly confirmed by data reported in Fig. 7, showing that emission from excited Si and H fragments lasts more than SiH and H_2 emission and terminates well after the end of the electronic current pulse. Production of high Rydberg fragments has been observed after dissociation of CH_4 by e-impact at energies above the 2nd IP [30] and the hydrogen fragment lifetimes were found in the range $1.0-0.5 \times 10^{-5}$ s. These values are of the same order of magnitude of H fragment emission lifetime observed in our experiment ($\geqq 5.0$ μs).

4. Final Product Analysis

Mass spectrometric analysis was performed on SiH_4 samples by an Extranuclear (Mod. 011-1) quadrupole mass spectrometer. Molecular hydrogen was the only significant gaseous product observed in mass spectrometric analysis of silane photolized samples. By adding 5 Torr of He as internal standard, we have verified that the silane loss in irradiated samples is accounted for by gaseous hydrogen formation in the ratio 1:2.

Disilane or higher silane formation was neither directly observed on the corresponding masses nor as a change in $Si^+/SiH^+/SiH_2^+/SiH_3^+$ relative intensities after laser photolysis.

A powdery deposit was observed both on the cell walls and cell windows after laser irradiation of silane. At low laser fluence ($\Phi \leqq 2$ J/cm^2), the onset for powder formation was found at $p \geqq 15$ Torr. A larger amount of dark brown powder was produced during sample irradiation at high laser fluences.

Infrared spectrophotometry of powders pressed in KBr pellets by a Perkin Elmer spectrophotometer (Mod. 283/2996) has shown the presence of small peaks corresponding to stretching ($\sim$2200–2100 cm^{-1}), bending (950–850 cm^{-1}) and wagging ($\sim$650 cm^{-1}) vibrational modes of silicon-hydrogen bonds.

The crystalline structure of the powders was evaluated using x-ray (CuKα) diffraction analysis. The x-ray diffraction patterns reveal three peaks corresponding to Si(111), (220), (311). The x-ray diffraction profile was also used to estimate the crystallinity of the samples since x-ray diffraction peaks of crystalline silicon are broadened by the characteristic background due to the amorphous phase, whenever present [34]. It has been found that the powders are mostly crystalline, the amorphous phase ($\sim$20–30%) being present only in Si powders obtained at low laser fluence.

All these results suggest the occurrence of the global reaction

$$SiH_4 \rightarrow Si\downarrow + 2\,H_2\uparrow . \tag{8}$$

Further details about final product analysis can be found in [34].

5. Conclusions

The mechanisms of CO_2 laser induced decomposition of silane at low and high laser fluences have been discussed on the basis of time and spectral dependence of luminescence emitted by excited photofragments.

At low laser fluence, the chemiluminescence observed in the range 420–880 nm has been attributed to emission from electronically excited states of SiH_2. Several studies indicate that the sylilene radical (SiH_2) is a key intermediate in a wide range of silane decomposition processes including pyrolysis [7], CVD [9, 35], glow-discharge [36] and ir laser induced dissociation [37–39]. But, at variance with other SiH_4 decomposition experiments, our final product analysis suggests the occurrence of a global reaction producing silicon rather higher silanes. We believe that the major feature which differentiates the gas phase reaction sequences following the homogeneous reaction (1) is the energy state in which the radical SiH_2 is formed. In fact, efficient molecular predissociation to $Si(^3P)+H_2$ is expected whenever SiH_2 is formed in the $^1B_1$ rovibronic states which are strongly coupled to $^3B_1$ levels, since the barrier to H_2 elimination is low for the $^3B_1$ manifold [15]. The subsequent steps are silicon particle nucleation and condensation. This reaction sequence is consistent with the global reaction (8) and with the absence of polysilanes in our final product analysis. On the other side, in all the experiments in which SiH_2 is formed in the ground state (i.e. silane pyrolysis and CVD [35], low fluence CO_2 laser induced silane dissociation [37, 38] ($\Phi \leqq 1$ J/cm^2), etc.)

SiH_2 insertion into unreacted silane giving rise to higher silanes is expected to be the dominant mechanism following the primary step (1).

At high laser fluences, silane breakdown takes place in the focal region at pressures above 3 Torr. In this regime, line optical spectra have been detected due to emission from mono and diatomic fragments formed in a silane plasma. All the emitting species (Si, SiH, H_2, H) are primary fragments of silane formed after dissociation from excited or superexcited (i.e. above the lowest IP at 18.2 eV) states.

The use of optical probes for plasma and CVD silane decomposition processes has already provided relevant information on the elementary reactions taking place in these systems. We have shown that in laser initiated decomposition processes, spectroscopic techniques can be even more valuable since the time evolution of elementary processes can be followed and new information can be obtained about the early stages of the photoreactions.

Acknowledgements. The authors wish to thank Prof. A. Giardini-Guidoni for stimulating discussions, Dr. R. Fantoni for having supplied data on mass spectrometric final product analysis and for precious suggestions, Dr. F. Pompa for x-ray diffraction analysis of powders; R. Belardinelli for his help in performing the measurements; P. Cardoni and G. Schina for their technical assistance.

References

1. Y. Hamakawa (ed.): *Amorphous Semiconductors – Technologies and Devices* (North-Holland, Amsterdam 1982)
2. D. Bäuerle (ed.): *Laser Processing and Diagnostics* (Springer, Berlin, Heidelberg 1984)
3. M.H. Brodsky (ed.): *Amorphous Semiconductors* (Springer, Berlin, Heidelberg 1979)
4. J.H. Purnell, R. Walsh: Proc. R. Soc. A **293**, 543 (1966)
5. R. Robertson, D. Hils, A. Gallagher: Chem. Phys. Lett. **103**, 397 (1984)
6. H.E. O'Neal, M.A. Ring: Chem. Phys. Lett. **107**, 442 (1984)
7. J.H. Purnell, R. Walsh: Chem. Phys. Lett. **110**, 330 (1984)
8. R. Viswanathan, D.L. Thompson, L.M. Raff: J. Chem. Phys. **80**, 4230 (1984)
9. M.E. Coltrin, R.J. Kee, J.A. Miller: J. Electrochem. Soc. **131**, 425 (1984)
10. J.F. O'Keefe, F.W. Lampe: Appl. Phys. Lett. **42**, 217 (1983)
11. T.F. Deutsch: J. Chem. Phys. **70**, 1187 (1979)
12. H. Reisler, C. Wittig: In *Photoselective Chemistry*, ed. by J. Jortner, R.D. Levine, S.A. Rice (Interscience, New York 1981) pp. 679–711
13. I. Dubois: Can. J. Phys. **46**, 2485 (1968)
14. a) J.W. Thoman, Jr., J.I. Steinfeld: Chem. Phys. Lett. **124**, 35 (1986)
    b) J.W. Thoman, Jr., J.I. Steinfeld, R. McKay, A.E.W. Knight: J. Chem. Phys. **86**, 5909 (1987)
15. M. Meunier, J.H. Flint, D. Adler, J.S. Haggerty: In *Laser Controlled Chemical Processing of Surfaces*, Mat. Res. Soc. Symp. Proc., Vol. 29, ed. by A. Wayne Johnson, D.J. Ehrlich (North-Holland, New York 1984)
16. J.L. Lyman, L.J. Radziemsky, Jr., A.C. Nilson: IEEE J. QE-**16**, 1174 (1980)
17. J.E. Rice, N.C. Handy: Chem. Phys. Lett. **107**, 365 (1984)
18. R.W. Pearse, A.G. Gaydon: *The Identification of Molecular Spectra* (Chapman and Hall, London 1965)
19. G. Olbrich: Chem. Phys. **101**, 381 (1986)
20. R.J. Glinsky, J.L. Gole, D.A. Dixon: J. Am. Chem. Soc. **107**, 5891 (1985)
21. D.M. Rayner, R.P. Steer, P.A. Hackett, C.L. Wilson, P. John: Chem. Phys. Lett. **123**, 449 (1986)
22. a) Y. Pauleau, D. Tonneau, G. Auvert: In *Laser Processing and Diagnostics*, ed. by D. Bäuerle (Springer, Berlin, Heidelberg 1984) pp. 215–220
    b) D. Tonneau, G. Auvert, Y. Pauleau: Chem. Phys. **103**, 353 (1986)
23. I. Oref: J. Chem. Phys. **75**, 131 (1982)
    I. Oref: J. Chem. Phys. **77**, 1253 (1982)
24. J. Steinwandel, J. Hoeschele: Chem. Phys. Lett. **116**, 25 (1985)
25. F.J. Kampas, R.W. Griffith: J. Appl. Phys. **52**, 1285 (1981)
26. "Tables of Spectral Lines" Zaidel', Prokof'ev, Slavnyi, Shreider (IFI/Plenum, New York 1970)
27. J. Perrin, J.F.M. Aarts: Chem. Phys. **80**, 351 (1983)
28. T. Sato, T. Goto: Jpn. J. Appl. Phys. **25**, 937 (1986)
29. A.W. Potts, W.C. Price: Proc. R. Soc. A **326**, 165 (1972)
30. T.G. Finn, B.L. Carnahan, W.C. Wells, E.C. Zipf: J. Chem. Phys. **63**, 1596 (1975)
31. Th. Heinis, K. Börlin, M. Jungen: Chem. Phys. Lett. **110**, 429 (1984)
32. M.A. Dillon, R.G. Wang, Z.W. Wang, D. Spence: J. Chem. Phys. **82**, 2909 (1985)
33. K. Börlin, Th. Heinis, M. Jungen: Chem. Phys. **103**, 83 (1986)
34. E. Borsella, L. Caneve, R. Fantoni: Proc. Workshop on Emerging Technologies for in Situ Processing, Cargese, 4–8 May 1987 (to be published as Nato ASI Series)
35. B.A. Scott, R.M. Placenik, E.E. Simonyi: Appl. Phys. Lett. **39**, 73 (1981)
36. B.A. Scott, M.H. Brodsky, D.C. Green, P.B. Kirby, R.M. Placenik, E.E. Simonyi: Appl. Phys. Lett. **37**, 725 (1980)
37. P.A. Longeway, F.W. Lampe: J. Am. Chem. Soc. **103**, 6813 (1981)
38. J.M. Jasinsky, R.D. Estes: Chem. Phys. Lett. **117**, 495 (1985)